

Multicomponent synthesis and investigations fluorescence activity of chromenone –pyrazole compounds

Ghods Mohammadi Ziarani (✉ gmziarani@hotmail.com)

Alzahra University <https://orcid.org/0000-0001-5177-7889>

Shirin Mohammadsaeed

Alzahra University

Alireza Badiei

Tehran University: University of Tehran

Jahan B. Ghasemi

Alzahra University

Research Article

Keywords: 4-Hydroxy-6-methyl-2H-pyran-2-one, Multiple-component reactions, Hydrazine derivative, Salicylaldehyde, Chromenone–Pyrazole compounds, Fluorescence compounds, Hg²⁺ Chemosensor

Posted Date: May 10th, 2021

DOI: <https://doi.org/10.21203/rs.3.rs-431208/v1>

License:   This work is licensed under a Creative Commons Attribution 4.0 International License.

[Read Full License](#)

Abstract

A synthetic method is described to produce some chromenone-pyrazole derivatives through a one-pot multicomponent reaction using $\text{SrFe}_{12}\text{O}_{19}$ as a magnetic catalyst. This method provides quite a few merits, including the use of an effective and easy separable nanocatalyst, high yields of products, short reaction time, and easy work-up. Two of the products showed fluorescence properties, which have detected mercury ions without any interference with other ions. They can detect a tiny amount of mercury ions, which were comparable with other chemosensors. The detection limit is 4×10^{-7} and 3×10^{-8} M, respectively, for the compound I and II, respectively, which were considered very low amounts. The effect of mercury on health and environmental pollution is essential in medical science.

Introduction

Coumarin is a familiar scaffold found in many natural products isolated from a wide range of species, especially plants. Dicoumarol is an anticoagulant agent that was discovered by Professor Link in 1933. This compound is a metabolized product of coumarin in the infected sweet clover (*Melilotus*) by some molds such as *Penicillium nigricans*. Warfarin is another important and famous coumarin derivative, which is used as an oral anticoagulant agent.¹ In addition to the pharmaceutical application of coumarin derivatives, some of them are beneficial sensors, such as 3-acetoacetyl coumarin (Fig. 1), which was used as a probe to find intracellular hydrazine in glioma cell lines because of the formation of a fluorescent coumarin-pyrazole product².

In recent years, a combination structure of coumarin and pyrazole has become an attractive scaffold in medicinal chemistry. Saeed *et al.* designed coumarinyl pyrazolinyl thioamide derivatives and determined their potential antioxidant activity against the urease enzyme.³

Among the various pyrazoles prepared by Wardakhan and Louca, coumarin-pyrazole compounds showed the highest activity against *Candida albicans*.⁴ Moreover, the antibacterial activity of quinolinepyrazoline-based coumarinyl thiazole derivatives has been assigned.⁵ Al-Ayed developed the synthesis of antioxidant coumarin containing a 4-arylbut-3-en-2-one moiety through the condensation of 3-acetyl coumarin with aryl aldehydes.⁶

Mercury pollution is one of the most challenging problems since its accumulation in the human body can lead to various neurological damages.⁷⁻⁸ Some industrial activities, including fossil-fuel combustion,⁹ gold mining,¹⁰ solid-waste burning,¹¹ and natural sources, such as forest fires and volcanic emissions¹² lead to rapid enhancement of Hg^{2+} levels in the environment. Additionally, ionic mercury can be converted to methylmercury naturally, which is more toxic than the mercury element and its salts.¹³ When methylmercury enters the environment, it results in bioaccumulation and high concentrations among populations of some species through the food chain.¹⁴ The Food and Drug Administration (FDA) and the United States Environmental Protection Agency (US EPA) advise the maximum allowable concentration

for methylmercury and mercury salts as 1 ppm (1 mg/L)¹⁵ and 2 ppb (0.002 mg/L),¹⁶ respectively. Hence, an appropriate and fast technique is essential to detect Hg²⁺. In recent years, extensive studies have been performed to develop sensitive and straightforward methods, such as resonating microcantilevers,¹⁷ voltammetry,¹⁸ colorimetric, and fluorescence spectroscopy¹⁹ for quick recognition of mercury ions.

In continuation of our research,²⁰⁻²³ herein a synthetic method for the synthesis of chromenone-pyrazole derivatives through a one-pot multicomponent reaction using SrFe₁₂O₁₉²⁴⁻²⁵ as a magnetic catalyst is described, and then the fluorescence properties of chromenone-pyrazole compounds against metal cations were investigated.

Experimental Section

General procedure for the preparation of the SrFe₁₂O₁₉ catalyst

SrFe₁₂O₁₉ magnetic nanoparticles (MNPs) were prepared by employing a simple sol-gel auto-combustion method, as reported before in literature.²⁶⁻²⁷

General procedure for the synthesis of coumarin-pyrazole derivatives (4a-g)

A combination of salicylaldehyde derivative **1** (1 mmol) and 4-hydroxy-6-methyl-2*H*pyran-2-one **2** (1 mmol, 0.13 g), and SrFe₁₂O₁₆ (0.02 g) was heated at the temperature of 120°C about approximately 15 min. Then, hydrazine (1 mmol) was added to the reaction mixture, which was stirred under the same conditions within (3–7 min) until reaction completion (traced by TLC method). Then, the raw product was dissolved in EtOAc, and the magnetic catalyst was separated using an external magnet. By evaporating the solvent, the product was precipitated out, and then crystals were filtered off, washed well with *n*-hexane, and then with water, respectively.

3-(3-Methyl-1*H*pyrazol-5-yl)-2*H*chromen-2-one (**4d**): Yield: 96%, yellow powder, mp: 182–184°C, FT-IR (KBr) ν_{\max} : 3427 (NH), 3037, 3091 (CH stretch), 1720 (-O-C = O), 1605 (C = N), 1576, 1474 (C = C), 1382 (CH₃) cm⁻¹, ¹H NMR (500 MHz, DMSO-*d*₆): 2.3 (s, 1H, CH₃), 6.7 (s, 1H, Pyrazole ring C-H), 7.3 (dd, 1H, Ar-H), 7.4 (d, 1H, Ar-H), 7.6 (t, 1H, Ar-H), 7.8 (s, 1H, Ar-H), 8.5 (s, 1H, Ar-H), 12.8 (s, 1H, NH) ppm. ¹³C NMR (125 MHz, DMSO-*d*₆): 10.9, 105, 115.83, 119.2, 124.5, 128.5, 131.3, 136.59, 152.63, 158.8 ppm

3-(3-Methyl-1-(4-nitrophenyl)-1*H*pyrazol-5-yl)-2*H*chromen-2-one (**4e**):

Yield: 97%, yellow powder, mp: 270–272°C, FT-IR (KBr) ν_{\max} : 3079 (CH stretch), 1741 (-O-C = O), 1599 (C = N), 1548, 1513, 1465 (C = C), 1384 (CH₃) cm⁻¹. ¹H NMR (500 MHz, DMSO-*d*₆): 2.3 (s, 3H, CH₃), 6.6 (s, 1H, Pyrazole ring C-H), 7.4 (t, 1H, Ar-H), 7.4 (d, 1H, Ar-H), 7.668 (t, 1H, Ar-H), 7.7 (d, 2H, Ar-H), 7.783 (d, 1H, Ar-H), 8.23 (d, 2H, Ar-H), 8.3 (s, 1H, Ar-CH) ppm. ¹³C NMR (125 MHz, DMSO-*d*₆): 13.2 (CH₃), 111.9, 116.2, 117.8, 118.7, 122.8, 124.8, 129.1, 132.7, 137.5, 144.2, 145.1, 145.2, 150.1, 153.5, 157.9 ppm.

5-Hydroxy-3-(3-methyl-1-phenyl-1*H*pyrazol-5-yl)-2*H*chromen-2-one (**4f**):

Yield: 96%, white powder, mp: 280–281°C, FT-IR (KBr) ν_{max} : 3415 (OH), 33070, 2923 (CH), 1684 (CO₂), 1605, 1585,, 1534 (C = C), 1374 (CH₃) cm⁻¹. ¹H NMR (500 MHz, DMSO-*d*₆): 2.3 (s, 3H, CH₃), 6.5 (s, 1H, Pyrazole ring C-H), 7.1 (d, 1H, Ar-H), 7.1 (d, 1H, Ar-H), 7.2 (t, 1H, Ar-H), 7.3 (m, 1H, Ar-H), 7.4 (m, 4H, Ar-H), 10.2 (s, 1H, Ar-H) ppm. ¹³C NMR (125 MHz, DMSO-*d*₆): 13.2 (CH₃), 109.9, 118.2, 118.8, 118.8, 119.5, 123.3, 124.8, 127.0, 129.1, 136.8, 140.3, 141.9, 144.0, 144.4, 148.3, 157.9 ppm.

6-Bromo-3-(3-methyl-1*H*pyrazol-5-yl)-2*H*chromen-2-one (**4g**):

Yield: 89%, yellow powder, mp: 241 – 239°C, FT-IR (KBr) ν_{max} : 3442 (NH), 3106, 2957 (CH), 1721 (CO₂), 1598 (C = N), 1566,1474, 1436 (C = C) cm⁻¹. ¹H NMR (125 MHz, DMSO-*d*₆): 2.3 (s, 3H, CH₃), 6.7 (s, 1H, Pyrazole ring C-H), 7.4 (d, 1H, Ar-H), 7.7 (d, 1H, Ar-H), 8.1 (s, 1H, Ar-CH), 8.5 (s, 1H, Ar-H) ppm. ¹³C NMR (125 MHz, DMSO-*d*₆): 9.9, 104.7, 115.8, 117.7, 120.9, 121.2, 133.1, 134.7, 138.8, 143.8, 151.3, 158.1 ppm.

Results And Discussion

Chromenone-pyrazole can be synthesized *via* a three-component reaction of salicylaldehydes **1**, 4-hydroxy-6-methyl-2*H*-pyron-2-one **2**, and phenylhydrazine **3**. Initially, the reaction conditions were optimized, and the results were shown in Table 1. Among the employed catalysts of SiO₂-Pr-SO₃H and SrFe₁₂O₁₉, in the case of the last one, the reaction time significantly reduced and gave the highest yield of product. This reaction was then investigated in the presence of SrFe₁₂O₁₉ magnetic catalyst in different solvents, including EtOH, H₂O, and a mixture of H₂O and EtOH, besides under solvent-free conditions. By comparing the obtained results, it was found that solvent-free condition at 120°C is the best condition in terms of reaction efficiency and time.

Afterward, this reaction was generalized with several salicylaldehydes and hydrazine compounds under the optimized conditions (Scheme 1), and the derivatives have been classified in Table 2. After completing the reaction (monitored by TLC), the raw product was dissolved in boiling EtOAc; furthermore, the catalyst was simply separated from the solution using a magnet, and the product was obtained via gradual solvent evaporation. The new products were characterized by melting point, FT-IR, GC-MS, and NMR spectral data. Melting points of synthesized derivatives were compared with data reported in the literature, as illustrated in Table 2.

The proposed mechanism for this reaction was presented in Scheme 2. At first, enol carbon of 4-hydroxy-6-methyl-2*H*-pyron-2-one **2** was added to the activated carbonyl group of salicylaldehyde **1** through the Knoevenagel condensation, and then the dehydration process gave the adduct product **6**, which is then cyclized intramolecularly to gain intermediate **7**. The dehydration process of compound **7** leads to the ring-opening of the pyran moiety to give chromenone **8**, which was reacted hydrazine compound **3**, followed by dehydration, cyclization, and another dehydration process to yield the final product **4**.

In comparison with the published methods in literature as shown in Table 3, the present methodology has several advantages such as the use of inexpensive magnetic catalyst, simple procedure, the short

reaction time, and the high purity of products. The nanomagnetic catalyst can be easily separated from the reaction mixture using an external magnet.

Investigation of fluorescence properties and sensitivity of chromenone-pyrazole compounds against metal cations

The fluorescence responses of chromenone-pyrazole derivatives were examined toward metal cations using fluorescence spectroscopy. As shown in Fig. 1, the fluorescence spectra of ethanolic solution of all derivatives (1×10^{-5} M) were recorded, and only **4d** and **4g** showed the fluorescence emission with $\lambda_{\text{ex}} = 348$ nm and $\lambda_{\text{em}} = 300$ nm, respectively. The presence of the aryl group on the nitrogen atom of the pyrazole group leads to the lack of fluorescence emission because the non-bonding electrons of the nitrogen atom participate in the resonance of the phenyl ring. Thus, the resonance energy of the pyrazole ring is decreased. Therefore, participating in the non-bonding electrons of the nitrogen atom in the pyrazole ring's resonance is essential for the product's fluorescence properties.

To investigate the interaction of various cations with compound **L₁**, Fe^{2+} , Fe^{3+} , Mn^{2+} , Mg^{2+} , Al^{3+} , Zn^{2+} , Cr^{3+} , Pb^{2+} , Co^{2+} , Hg^{2+} , K^+ , Ca^{2+} , Cu^{2+} , Cd^{2+} and Ag^+ cations (100 μL , 0.01 M) were separately added to the ethanolic solution of **L₂** (3 mL, 10^{-5} M) and the changes were indicated at the emission wavelength of 418 nm. The intensity of emission peak was decreased significantly only in the presence of Hg^{2+} as shown in Fig. 2.

To explore the selectivity of the **L₁** against mercury ions, competitive experiments were performed against other metal cations (Fe^{2+} , Fe^{3+} , Ca^{2+} , Cd^{2+} , Mn^{2+} , Co^{2+} , Pb^{2+} , Cu^{2+} , Ag^+ , Mg^{2+} , Ni^{2+} , Cr^{3+} , Zn^{2+} , Na^+ , Al^{3+} and K^+). As shown in Fig. 3, no significant interference is observed, and therefore, it can be claimed that compound **L₁** is a selective fluorescence chemosensor for the discernment of mercury ions even in the presence of other metal cations.

Titration experiment was accomplished in absolute EtOH solution of **L₁** with different amounts of Hg^{2+} . As shown in Fig. 4, the emission of chemosensor **L₁** regularly decreases by increasing Hg^{2+} concentration. The Fig. 4 inset shows good linear relations between the emission at 418 nm and the concentration of Hg^{2+} with the linear equation of emission = $-218.96 [\text{Hg}^{2+}] + 609.12$ in the equivalent range and $R^2 = 0.987$. The detection limit for chemosensor **L₁** to detect mercury has been found from the following equation: $\text{DL} = (kS_d)/m$, where k is a constant factor equal to 3, S_d is the standard deviation obtained from the determination of the sample emission intensity at 412 nm for 6 replicates, and m is the slope of emission intensity against Hg^{2+} concentration. So the detection limit of **L₁** for Hg^{2+} was calculated as 4×10^{-7} M.

Another derivative of 6-bromo-chromenone-pyrazole (**L₂**), also represents fluorescence properties. Thus, the effect of cation on the fluorescence properties of **L₂** was also investigated. The ligand's interaction was selective toward mercury ions because a sharp decrease is observed after adding a certain aliquot of

Hg²⁺ solution (Fig. 5). Therefore, the effect of interfering ions was then studied to explore the selectivity of **L**₂ for the detection of mercury ions. Fortunately, any of the cations did not interfere with L2-Hg²⁺ (Fig. 6).

The titration experiment for **L**₂ was accomplished as the same **L**₁ (Fig. 7). The emission of chemosensor **L**₂ again decreases by the gradually increasing amount of Hg²⁺. The inset in (Fig. 7) shows a well linear relation between the emission at 426 nm and the concentration of Hg²⁺ with the linear equation of emission = -275.01[Hg²⁺] + 346.23 and R² = 0.9899. The detection limit was also calculated like the method mentioned above and was **L**₂ 3 × 10⁻⁸ M. **Fig. 7:** Fluorescence emission of chemosensor **L**₂ upon addition of Hg²⁺ ions in absolute EtOH solution; Inset: plot of fluorescence emission as a function of Hg²⁺ concentration.

The presented compounds have shown very distinct advantages over the previously reported compounds in the detection and measurement of mercury ions. The analytical performance of mercury ions' current chemosensor and some of the significant reported methods are summarized in Table 3. One of the essential factors in the synthesis of new compounds 1, 2, and 3 is using a green solvent. In this regard, EtOH is an undoubtedly better solvent than CH₃CN. Compound 3 showed an excellent detection limit, but the synthesis method was complicated. In the case of compound **5**, while the applied solvent DMF is poisonous, the obtained detection limit is remarkably lower than the reported one. For compounds **6** and **7** as novel fluorescence sensors with excellent detection limit, a simple, green, and short time synthesis method was reported.

Conclusions

In summary, the chromenone-pyrazoles derivatives were synthesized by the multicomponent reaction approach in solvent-free conditions using a nanomagnetic catalyst. Among the seven derivatives, only two compounds have had fluorescence properties and responded to the Hg²⁺ ion with the low detection limit. The two fluorescent compounds in the pyrazole group have not aromatic groups. Then, *N* group is the main factor in generating the fluorescence property of these compounds.

Declarations

Acknowledgments: The authors are thankful to the research council of Alzahra University.

Declarations: There is no conflict of interest.

Data Availability: The supporting information is available on the Springer publication website.

Funding: This research did not receive any specific grant from funding agencies in the public, commercial, or not-for-profit sectors.

Declarations Ethics Approval: Not applicable

Consent to Participate: Not applicable.

Consent for Publication: Not applicable.

Authors' Contributions

Ghodsii Mohammadi Ziarani: Corresponding author, concept design, Review writing and editing.

Shirin Mohammadsaeed: concept design, editing, Performed the experiments and modification.

Alireza Badii: Contributed reagents, materials, Review modification, editing, and analysis data.

Jahan B. Ghasemi: Review modification, editing, and Analyzed and interpreted the data.

References

1. Reynolds, M. W.; Fahrbach, K.; Hauch, O.; Wygant, G.; Estok, R.; Cella, C.; Nalysnyk, L., Warfarin anticoagulation and outcomes in patients with atrial fibrillation: a systematic review and metaanalysis. *Chest* 2004, 126 (6), 1938-1945.
2. Wu, W.-N.; Wu, H.; Wang, Y.; Mao, X.-J.; Zhao, X.-L.; Xu, Z.-Q.; Fan, Y.-C.; Xu, Z.-H., A highly sensitive and selective off–on fluorescent chemosensor for hydrazine based on coumarin β -diketone. *Spectrochimica Acta Part A: Molecular and Biomolecular Spectroscopy* 2018, 188, 80-84.
3. Saeed, A.; Mahesar Parvez, A.; Channar Pervaiz, A.; Larik Fayaz, A.; Abbas, Q.; Hassan, M.; Raza, H.; Seo, S. Y., Hybrid Pharmacophoric Approach in the Design and Synthesis of Coumarin Linked Pyrazolinyl as Urease Inhibitors, Kinetic Mechanism and Molecular Docking. *Chemistry & Biodiversity* 2017, 14 (8), e1700035.
4. Wardakhan, W. W.; Louca, N. A., Synthesis of novel pyrazole, coumarin and pyridazine derivatives evaluated as potential antimicrobial and antifungal agents. *Journal of the Chilean Chemical Society* 2007, 52, 1145-1149.
5. Ansari, M. I.; Khan, S. A., Synthesis and antimicrobial activity of some novel quinoline-pyrazoline-based coumarinyl thiazole derivatives. *Medicinal Chemistry Research* 2017, 26 (7), 1481-1496.
6. Al-Ayed, A. S., Synthesis of New Substituted Chromen[4,3-c]pyrazol-4-ones and Their Antioxidant Activities. *Molecules* 2011, 16 (12), 10292.
7. Baughman, T. A., Elemental mercury spills. *Environmental Health Perspectives* 2006, 114 (2), 147-152.
8. Fitzgerald, W. F.; Lamborg, C. H.; Hammerschmidt, C. R., Marine biogeochemical cycling of mercury. *Chemical Reviews* 2007, 107 (2), 641-662.

9. Wang, Q.; Shen, W.; Ma, Z., Estimation of mercury emission from coal combustion in China. *Environmental Science & Technology* 2000, 34 (13), 2711-2713.
10. Malm, O., Gold mining as a source of mercury exposure in the Brazilian Amazon. *Environmental Research* 1998, 77 (2), 73-78.
11. Vogg, H.; Braun, H.; Metzger, M.; Schneider, J., The specific role of cadmium and mercury in municipal solid waste incineration. *Waste Management & Research* 1986, 4 (1), 65-73.
12. Biswas, A.; Blum, J. D.; Klaue, B.; Keeler, G. J., Release of mercury from Rocky Mountain forest fires. *Global Biogeochemical Cycles* 2007, 21 (1), 1-13.
13. Bailey, J. M.; Davidson, N., Methylmercury as a reversible denaturing agent for agarose gel electrophoresis. *Analytical Biochemistry* 1976, 70 (1), 75-85.
14. Harada, M., Minamata disease: Methylmercury poisoning in Japan caused by environmental pollution. *Critical Reviews in Toxicology* 1995, 25 (1), 1-24.
15. FDA, An exposure assessment for methylmercury from seafood for consumers in the United States; <http://www.fda.gov/downloads/Food/FoodborneIllnessContaminants/UCM114740.pdf>.
16. EPA, U. Human health criteria - methylmercury; <https://www.epa.gov/wqc/human-health-criteria-methylmercury>.
17. Thundat, T.; Wachter, E. A.; Sharp, S. L.; Warmack, R. J., Detection of mercury vapor using resonating microcantilevers. *Applied Physics Letters* 1995, 66 (13), 1695-1697.
18. Salaün, P.; van den Berg, C. M. G., Voltammetric detection of mercury and copper in seawater using a gold microwire electrode. *Analytical Chemistry* 2006, 78 (14), 5052-5060.
19. Afshani, J.; Badiei, A.; Karimi, M.; Lashgari, N.; Mohammadi Ziarani, G., A single fluorescent sensor for Hg²⁺ and discriminately detection of Cr³⁺ and Cr(VI). *Journal of Fluorescence* 2016, 26 (1), 263-270.
20. Mohajer, F.; Mohammadi Ziarani, G.; Badiei, A.; Ghasemi, J. B., SBA-Pr-Imine-Furan as an environmental adsorbent of Pd(II) in aqueous solutions. *Environmental Challenges* 2021, 3, 100032.
21. Mohammadi Ziarani, G.; Ebrahimi, Z.; Mohajer, F.; Badiei, A., A fluorescent chemosensor based on functionalized nanoporous silica (SBA-15 SBA-IC-MN) for detection of Hg²⁺ in aqueous media. *Arab. J. Sci. Eng.* 2021.
22. Mohammadi Ziarani, G.; Akhgar, M.; Mohajer, F.; Badiei, A., SBA-Pr-IS-MN synthesis and its application as Ag⁺ optical sensor in aqueous media. *Res. Chem. Intermed.* 2021.
23. Mohammadi Ziarani, G.; Khademi, M.; Mohajer, F.; Badiei, A., The application of modified SBA-15 as a chemosensor. *Curr. Org. Chem.* 2021.
24. Kheilkordi, Z.; Mohammadi Ziarani, G.; Bahar, S.; Badiei, A., The green synthesis of 2-amino-3-cyanopyridines using SrFe₁₂O₁₉ magnetic nanoparticles as efficient catalyst and their application in complexation with Hg²⁺ ions. *J. Iran. Chem. Soc.* 2019, 16 (2), 365-372.
25. Ahmadi, T.; Mohammadi Ziarani, G.; Masoumian Hoseini, S. M.; Badiei, A.; Ranjbar, M. M., Synthesis, characterization, and molecular docking of benzodiazepines in the presence of SrFe₁₂O₁₉ magnetic nanocatalyst. *J. Iran. Chem. Soc.* 2021.

26. Mohammadi Ziarani, G.; Kazemi Asl, Z.; Gholamzadeh, P.; Badiei, A.; Afshar, M., The use of SrFe₂O₇ magnetic nanoparticles as an efficient catalyst in the modified Niementowski reaction. *Applied Organometallic Chemistry* 2017, 31 (12), e3830.
27. Mohammadi Ziarani, G.; Kazemi Asl, Z.; Gholamzadeh, P.; Badiei, A.; Afshar, M., Sol-gel auto-combustion production of SrFe₂O₇ magnetic nanoparticles and its application in the synthesis of spirooxindol-quinazolinone derivatives. *Journal of Sol-Gel Science and Technology* 2018, 85 (1), 103-109.
28. Alizadeh, A.; Ghanbaripour, R., Synthesis of 3-(3-Methyl-1-aryl-1 H-pyrazol-5-yl)-2 H-2-chromen-2-one Derivatives via a One-Pot, Three-Component Reaction. *Synthetic Communications* 2014, 44 (11), 1635-1640.
29. Li, X.-T.; Liu, Y.-H.; Liu, X.; Zhang, Z.-H., Meglumine catalyzed one-pot, three-component combinatorial synthesis of pyrazoles bearing a coumarin unit. *RSC Advances* 2015, 5 (33), 25625-25633.
30. Choi; Kim, J.-Y.; Yoon, W.-T.; Ju-Young, Bull. Korean. Chem. Soc. 2012, 33 (7), 2359-2364.
31. Martinez, R.; Espinosa, A.; Tarraga, A.; Molina, P., *Tetrahedron*. 2010, 66 (22), 3662-3667.
32. Chen, Q.-Y.; Chena, C.-F., *Tetrahedron Lett.* 2005, 46 (1), 165-168.
33. Caballero, A.; Martinez, R.; Lloveras, V.; Ratera, I.; Vidal-Gancedo, J.; Wurst, K.; Tarraga, A.; Molina, P.; Veciana, J., *J. Am. Chem. Soc.* 2005, 127 (45), 15666-15667.
34. Erdemir, S.; Kocyigit, O.; Karakurt, S., *Sens. Actuators. B. Chem.* 2015, 220, 381-388.

Tables

Due to technical limitations the Tables are available as a download in the Supplementary Files.

Figures

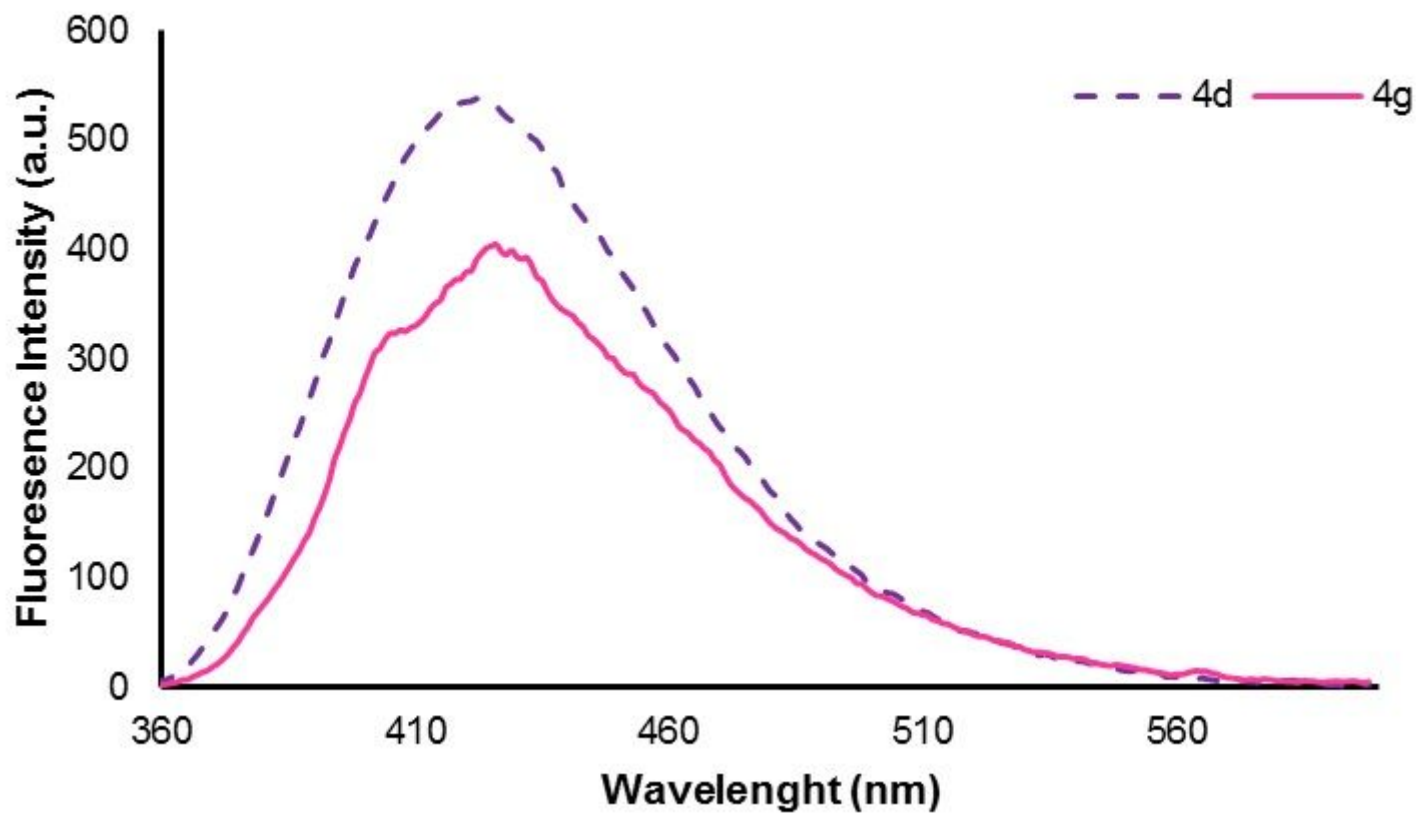


Figure 1

Fluorescence emission of chromenone-pyrazole 4d (L1) and 4g (L2)

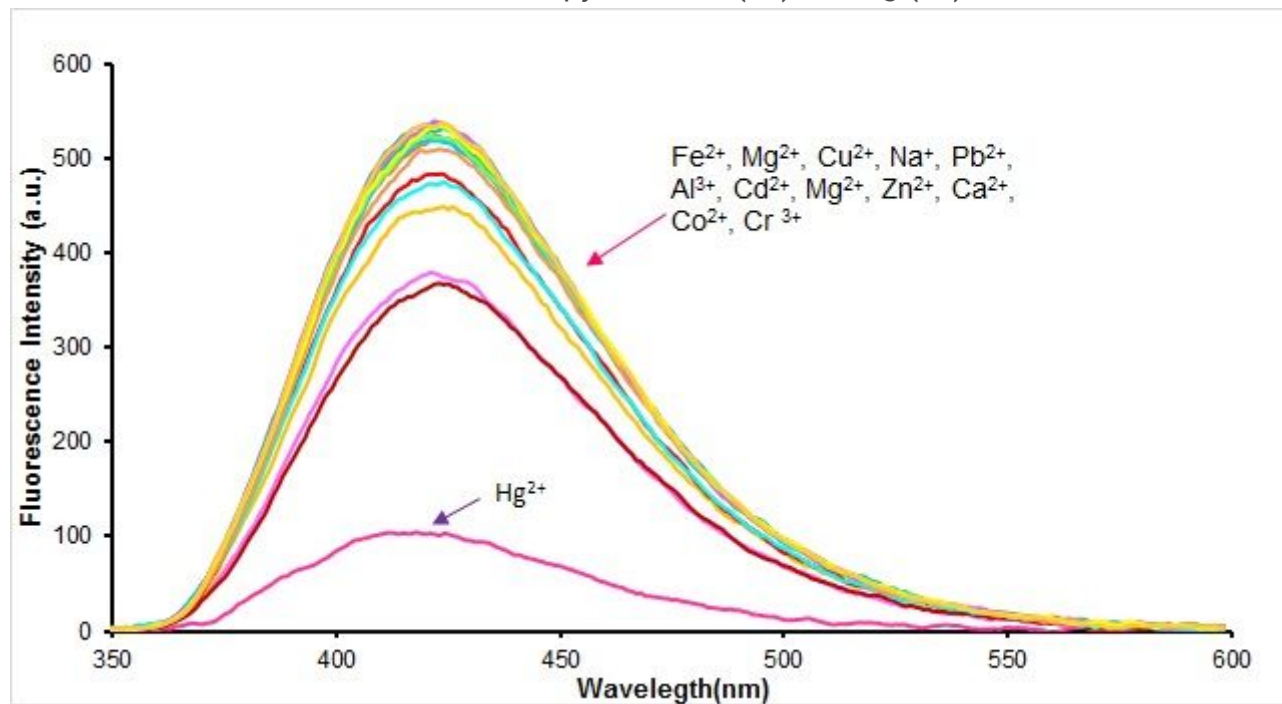


Figure 2

Fluorescence emission for a new compound of L1 in the presence of 100 μL (0.01 M) of metal cations (Ca^{2+} , Cd^{2+} , Co^{2+} , Pb^{2+} , Cu^{2+} , Ag^{+} , Mg^{2+} , Ni^{2+} , Hg^{2+} , Zn^{2+} , Al^{3+} , K^{+} , Hg^{2+}) in absolute ethanol ($\lambda_{\text{ex}} = 300 \text{ nm}$ and $\lambda_{\text{em}} = 334 \text{ nm}$).

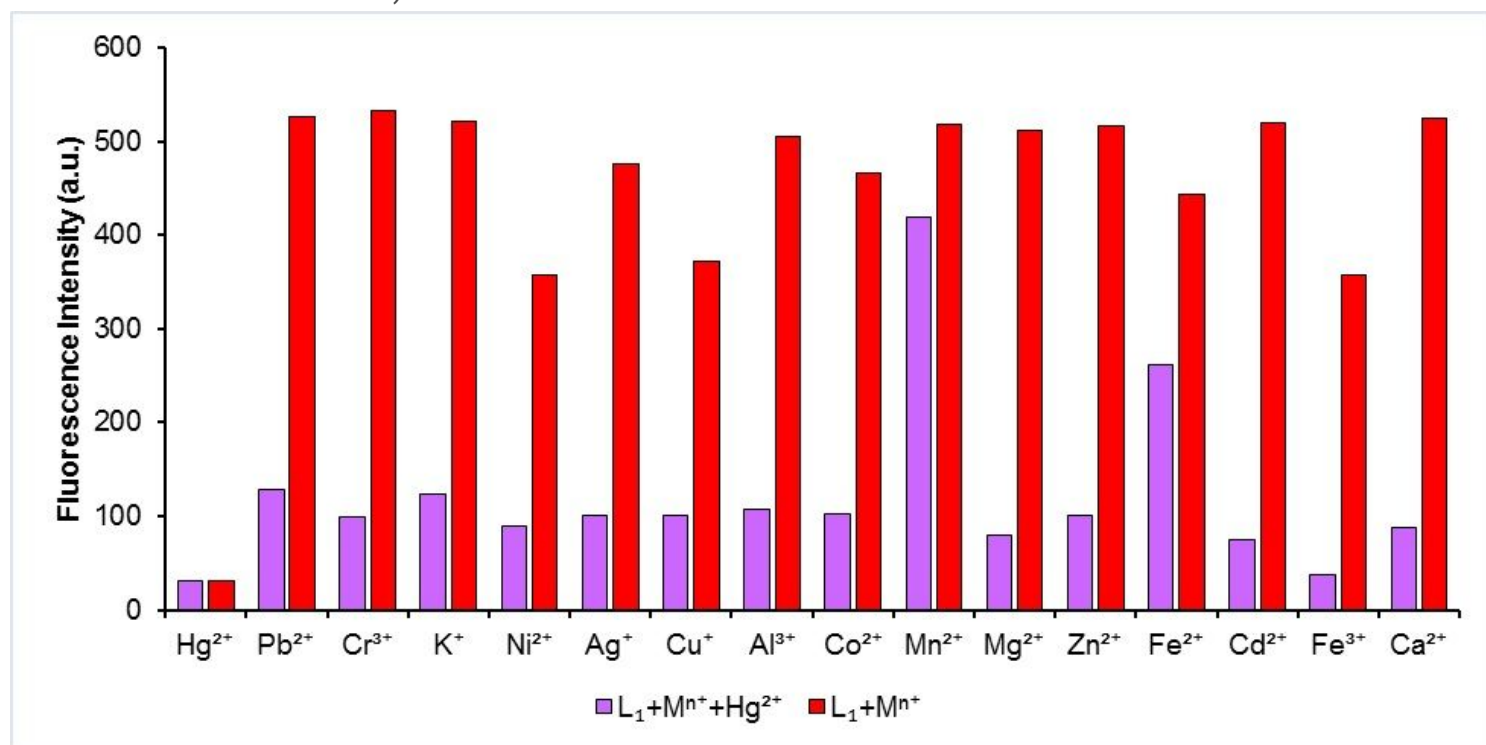


Figure 3

Selectivity of chemosensor L1 for Hg^{2+} against other metal cations in an ethanolic solution ($\lambda_{\text{ex}} = 300 \text{ nm}$ and $\lambda_{\text{em}} = 334 \text{ nm}$).

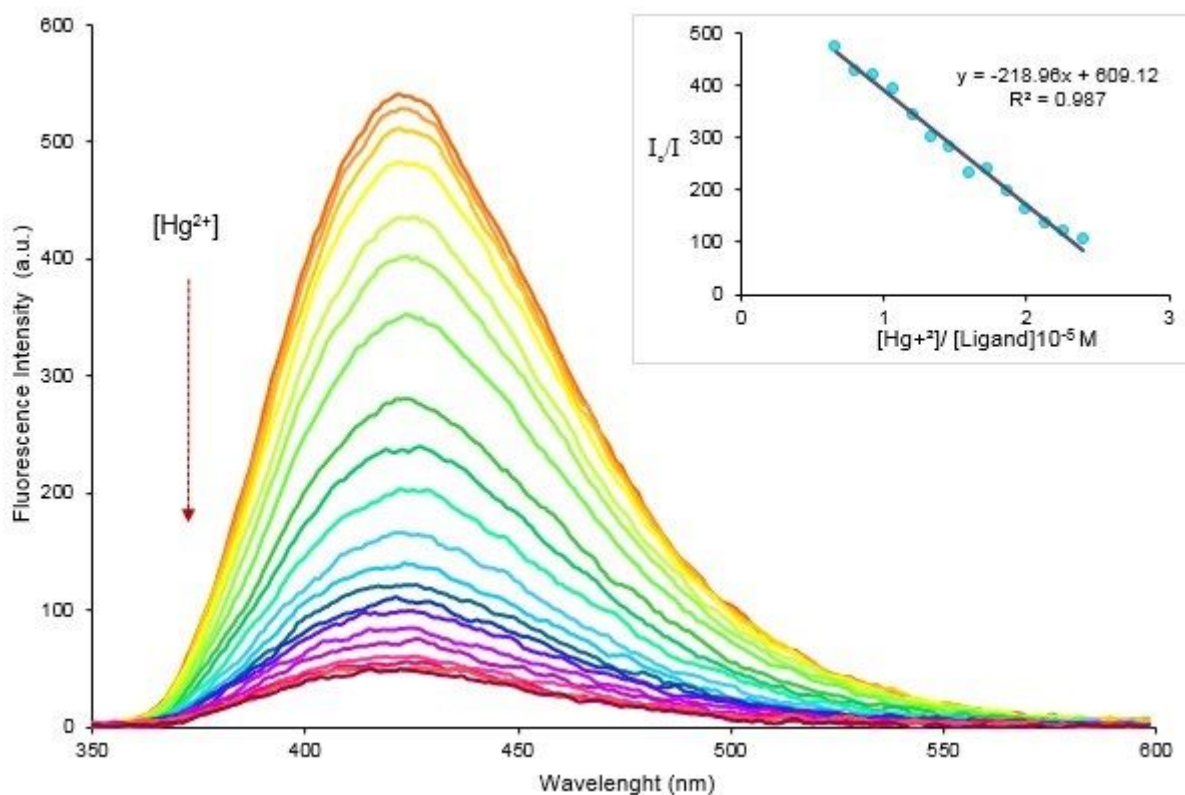


Figure 4

Fluorescence emission of chemosensor L1 over addition of Hg^{2+} in EtOH absolute solution; inset: plot of fluorescence emission as a function of Hg^{2+} concentration ($\lambda_{\text{ex}} = 300 \text{ nm}$ and $\lambda_{\text{em}} = 334 \text{ nm}$).

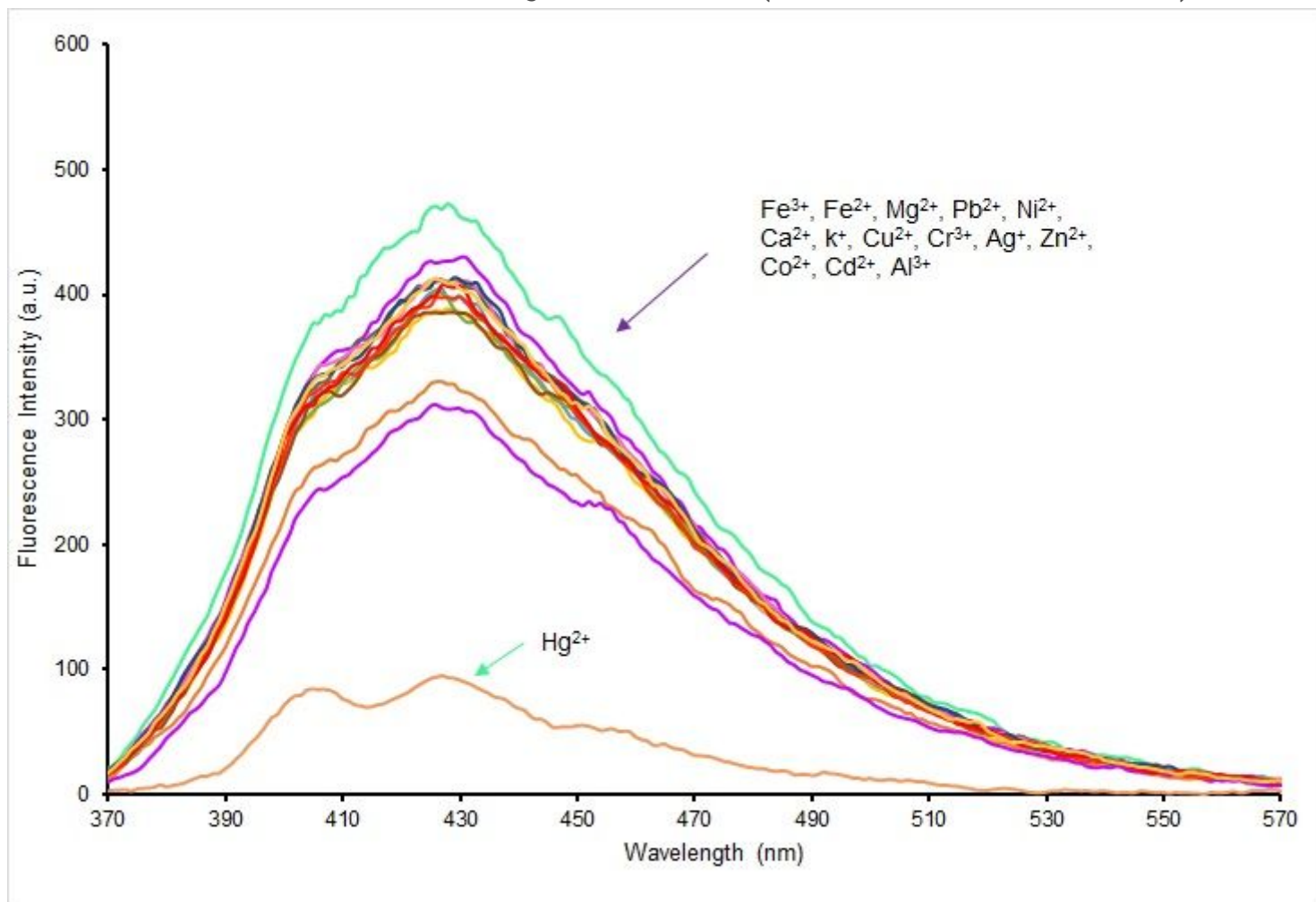


Figure 5

Fluorescence emission of chemosensor L2 in the presence of several metal cations (Fe^{3+} , Fe^{2+} , Cd^{2+} , Co^{2+} , Cr^{3+} , Cu^{2+} , Ag^+ , K^+ , Al^{3+} , Zn^{2+} , Pb^{2+} , Mg^{2+} , Hg^{2+} , Ca^{2+} , Ni^{2+}) in absolute EtOH, $\lambda_{\text{ex}} = 300$ and $\lambda_{\text{em}} = 348$

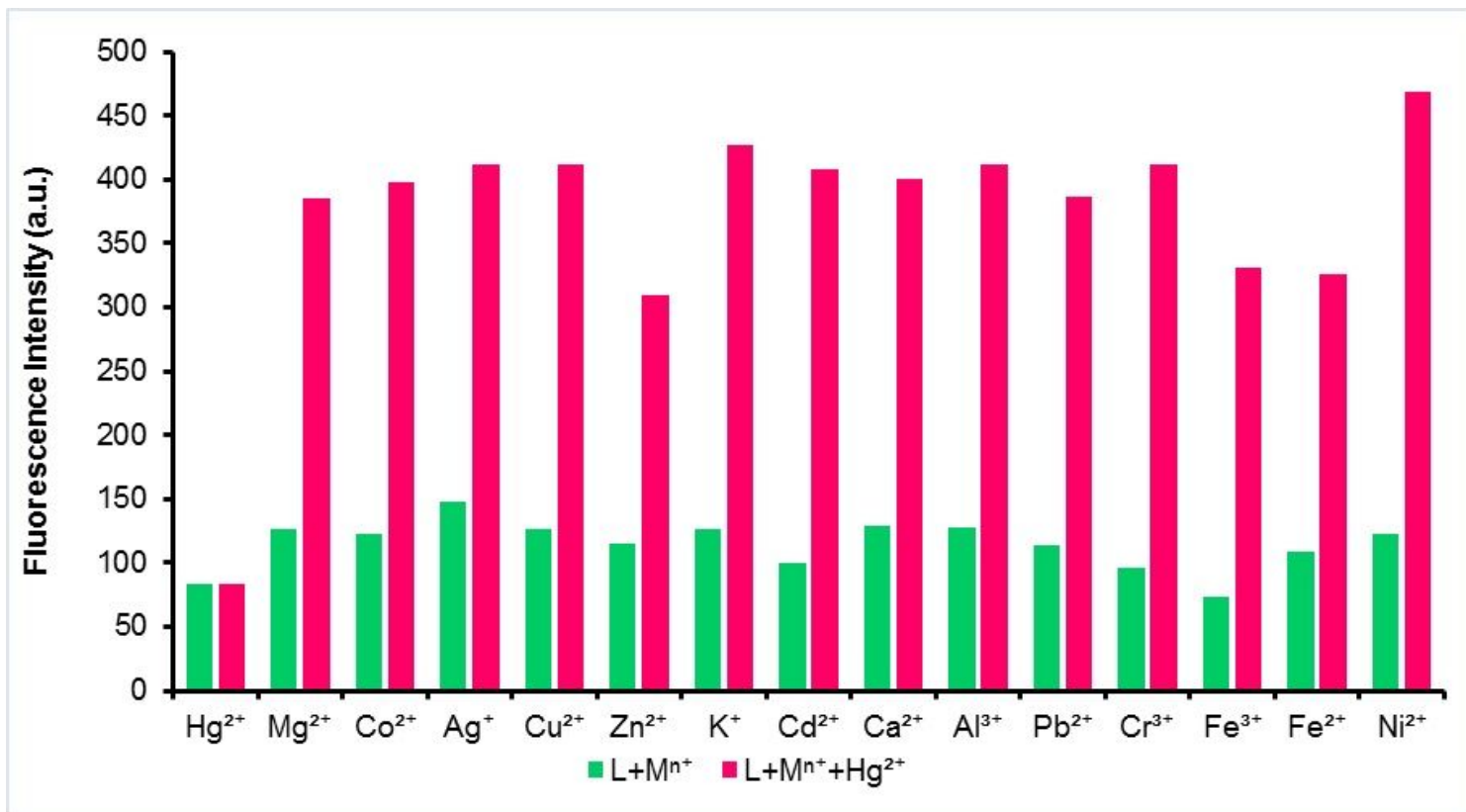


Figure 6

Selectivity of chemosensor 4g (3mL) for Hg²⁺ (100μL, 1×10⁻³ M) in the presence of metal cations in an absolute ethanol solution, (λ_{ex}=300, λ_{em}=348)

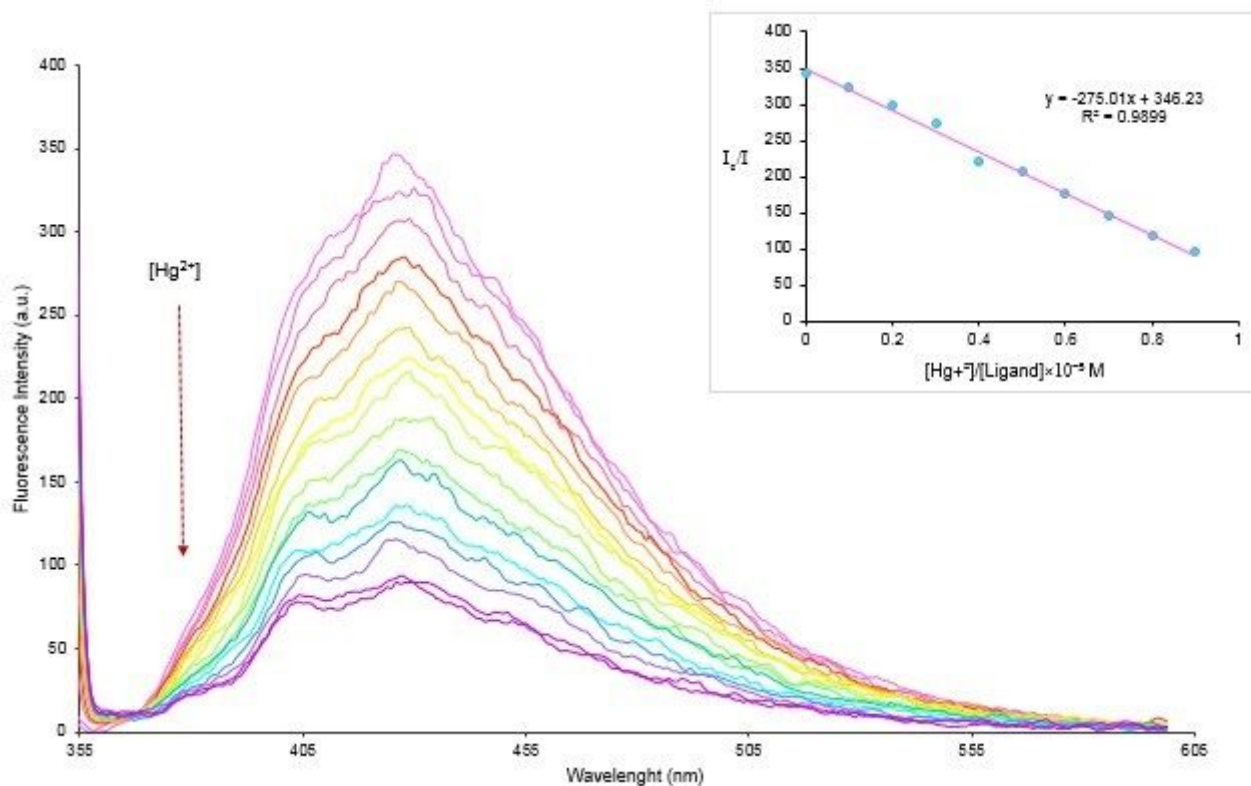


Figure 7

Fluorescence emission of chemosensor L2 upon addition of Hg²⁺ ions in absolute EtOH solution; Inset: plot of fluorescence emission as a function of Hg²⁺ concentration.

Supplementary Files

This is a list of supplementary files associated with this preprint. Click to download.

- [Tables.pdf](#)
- [Schemes.pdf](#)